Model for stress and volume changes of a thin film on a substrate upon annealing: Application to amorphous Mo/Si multilayers

O. B. Loopstra, E. R. van Snek, Th. H. de Keijser, and E. J. Mittemeijer
Laboratory of Metallurgy, Delft University of Technology, Rotterdamseweg 137, 2628 AL Delft, The Netherlands
(Received 23 August 1991)

A model is given for the stress change in a thin film on a thick substrate during annealing. It takes into account temperature changes, volume changes, viscous flow, and anelastic relaxation occurring in the film. The stress change in amorphous Mo/Si multilayer films deposited on Si single-crystal substrates was obtained from *in situ* wafer-curvature measurements during annealing at temperatures below the glass temperature. The thickness change and the interdiffusion coefficient were obtained from the position and the intensity of the first-order multilayer x-ray reflection. The unconstrained volume change was derived from the measured stress and thickness changes. The free-volume model for amorphous solids has been used to interpret the interdiffusion in and the volume change of the amorphous Mo/Si multilayers. The stress change as it occurred during isothermal annealing was explained by free-volume annihilation, viscous flow, and anelastic relaxation. If anisotropy of the volume change is accepted, the stress change could also be described with free-volume annihilation and viscous flow alone. The product of the experimentally observed viscosity and diffusion coefficient for amorphous Mo/Si multilayers was compared to the value expected from the free-volume-model-based equivalent of the Stokes-Einstein relation.

I. INTRODUCTION

If a thin film is rigidly fixed on a relatively thick substrate, the lateral dimensions of the film are defined by the substrate. Then, a volume change of the film will result in a buildup of mechanical stress. Such volume changes can be caused by a change of molar volume in the film or a change of temperature. Viscous flow and anelastic relaxation of the film can also change the mechanical stress.

In this paper a model is presented for the stress changes in a thin film on a thick substrate upon annealing. The model is tested by using stress and film thickness data obtained during diffusion annealing below the glass temperature of amorphous Mo/Si multilayers on a Si single-crystal substrate.

Stresses in the amorphous multilayer have been determined by measuring *in situ* the substrate curvature. The film thickness change has been obtained from the change of the x-ray diffraction angle of the first-order reflection corresponding to the composition modulation of the multilayer. The unconstrained volume change of the film has been derived from these stress and thickness changes. The time-dependent interdiffusion coefficient has been determined from the integrated intensity of the first-order multilayer reflection, measured as a function of annealing time.

After production of an amorphous solid its so-called free volume is usually much larger than the equilibrium amount of free volume. During annealing the excess free volume is annihilated as part of a process called structural relaxation. The associated changes of physical properties of amorphous solids, like viscosity, density, and diffusion coefficient, have been described previously with the "free-volume model."[1] From that a relation between viscosity and diffusion coefficient similar to the Stokes-Einstein relation for liquids has been derived.[1]

The present experimental stress, volume, and interdiffusion data have been explained in terms of the free-volume model. Since both the viscosity and the diffusion coefficient have been obtained from one specimen, this investigation additionally provides an opportunity to test the free-volume-model-based equivalent of the Stokes-Einstein relation for amorphous solids.

II. STRESS AND VOLUME CHANGE

If a film is rigidly fixed on a substrate, the lateral dimensions of the film cannot be changed independently from the dimensions of the substrate. Usually the thickness of the substrate exceeds the thickness of the film many times. Then, any lateral misfit between film and substrate is accommodated fully by the film with elastic or plastic deformation. Therefore any process that changes the lateral dimensions of an unconstrained thin film gives rise to a change of stress of that thin film when fixed on a thick substrate.

Stresses in amorphous thin films on a substrate can be changed by (i) thermal expansion/shrinkage, (ii) change of volume of the layer, (iii) viscous flow, and (iv) anelastic relaxation; see Fig. 1. In the following a model will be presented that describes the temperature-time behavior of the stress in an amorphous thin film on a thick substrate as a result of the four processes mentioned; see Sec. II E.

A change of stress in the thin film also leads to a change of thickness of the film. To obtain the unconstrained *volume* change of an amorphous thin film on a thick substrate the measured thickness change must be

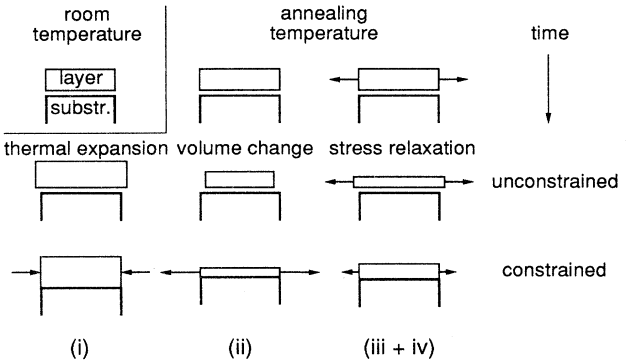

FIG. 1. Schematic representation of stress and thickness changes for a thin film on a thick substrate. (i) Thermal expansion. (ii) Change of specific volume. (iii+iv) Stress relaxation due to viscous flow and/or anelastic relaxation.

corrected for the change of stress in the film; see Sec. II F below.

The (amorphous) layer is considered to be elastically isotropic. The state of stress in the layer is taken to be biaxial such that both principal stresses are equal and in the plane of the layer. The subscript $\parallel$ is used to indicate stress and strain components parallel to the surface, the subscript $\perp$ is used for strain components perpendicular to the surface (the stress perpendicular to the surface is zero). Elastic strains (deformations) will be denoted by the symbol ε, whereas plastic strains (deformations) will be denoted by the symbol e. Stresses will be denoted by the symbol σ; see Fig. 2.

It is normally taken for granted that plastic deformations do not change the volume.[2] Hence

$$e_\perp = -2e_\parallel \ . \tag{1}$$

The relation between the (elastic) strains perpendicular and parallel to the plane of the layer is

$$\varepsilon_\perp = \frac{-2\nu_l}{1-\nu_l}\varepsilon_\parallel \ , \tag{2}$$

where ν_l is the Poisson constant of the layer.

Since the layer is rigidly fixed to the substrate, the lateral dimensions of the layer cannot change. Hence, at any time t, the sum of the lateral elastic and plastic strains is equal to the initial elastic strain

$$\varepsilon_\parallel + e_\parallel = \varepsilon_\parallel(t=0) \ . \tag{3}$$

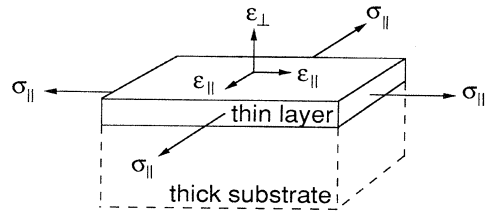

FIG. 2. Definitions of symbols used to describe stresses and strains in a thin film on a thick substrate.

In differential form

$$\frac{de_\parallel}{dt} = -\frac{d\varepsilon_\parallel}{dt} \ . \tag{4}$$

The relation between the stress and the (elastic) strain parallel to the plane of the layer is

$$\sigma_\parallel = \frac{E_l}{1-\nu_l}\varepsilon_\parallel \ , \tag{5}$$

where E_l is the modulus of elasticity of the layer.

A. Strain change by thermal misfit

If the linear thermal expansion coefficients of the substrate and the thin film differ, a temperature change will result in buildup of a "thermal" strain, which in case of elastic accommodation satisfies

$$(\varepsilon_\parallel)_{\rm th} = -\int_{T_1}^{T_2}(\alpha_l - \alpha_s)dT \ , \tag{6}$$

where $(\varepsilon_\parallel)_{\rm th}$ is the thermal strain in the layer, T_1 and T_2 are the beginning and ending temperatures, respectively, and α_l and α_s are the linear expansion coefficients of layer and substrate, respectively. Assuming $\Delta\alpha_{\rm th} = (\alpha_l - \alpha_s)$ to be temperature independent, the thermal strain change rate is proportional to the temperature change rate according to

$$\left[\frac{d\varepsilon_\parallel}{dt}\right]_{\rm th} = -\Delta\alpha_{\rm th}\frac{dT}{dt} \ . \tag{7}$$

B. Strain change by volume change of the layer

During annealing the volume of an unconstrained amorphous layer can change by several causes: (i) change of average atomic volume due to mixing, (ii) release of gases incorporated during layer production, (iii) annihilation of free volume. The change of unconstrained volume is supposed to be isotropic and stress independent. The relative volume change rate in directions parallel and perpendicular to the unconstrained layer equals $(\frac{1}{3})dv(t)/dt \equiv (\frac{1}{3})[1/V(t=0)]dV(t)/dt$, where V is the volume of the layer. Since the lateral dimensions of the film are determined by the substrate, this causes a buildup of lateral elastic strains. With Eq. (4) one obtains

$$\left[\frac{d\varepsilon_\parallel}{dt}\right]_{\rm vol} = -\frac{1}{3}\frac{dv}{dt} \ . \tag{8}$$

C. Strain change by viscous flow

Relaxation of elastic stresses (strains) can be brought about by viscous flow. For thin films in the state of plane stress described above, the viscosity η is defined according to[3]

$$\eta = \frac{\sigma_\parallel}{6\left[\frac{de_\parallel}{dt}\right]} \ . \tag{9}$$

From Eqs. (4) and (9) it follows for the elastic strain change rate

$$\left[\frac{d\varepsilon_{\parallel}}{dt}\right]_{\text{flow}} = -\frac{\sigma_{\parallel}}{6\eta} . \tag{10}$$

D. Strain change by anelastic relaxation

It is well known that in amorphous solids anelastic relaxation (stress-induced ordering) can occur.[4,5] In a thin film on a substrate the strain change caused by anelastic relaxation $(d\varepsilon_{\parallel}/dt)_{\text{anel}}$ will lead to a stress change too. At constant applied stress or strain the kinetics of anelastic relaxation in amorphous solids is already complicated. For its description spectra of activation energies have been adopted.[6] Furthermore, in an amorphous thin film on a substrate neither the (applied) stress nor the strain are constant because of the simultaneously occurring annihilation of free volume, viscous flow, and anelastic relaxation.

E. Total stress change

The infinitesimal elastic strain changes due to the processes described in Secs. II A–II D will be considered as additive. If E_l and ν_l are assumed to be time and temperature independent, then the differential equation describing the stress change rate in an amorphous thin film on a thick substrate during heat treatment at temperatures below the glass transition temperature is obtained from Eqs. (7), (8), (10), and the differential form of Eq. (5) as

$$\frac{d\sigma_{\parallel}}{dt} = -\frac{E_l}{1-\nu_l}\left[\Delta\alpha_{\text{th}}\frac{dT}{dt} + \frac{1}{3}\frac{dv}{dt} + \frac{\sigma_{\parallel}}{6\eta} - \left[\frac{d\varepsilon_{\parallel}}{dt}\right]_{\text{anel}}\right] . \tag{11}$$

Note that η is time dependent (cf. Sec. III).

F. Volume change

The change rate of the relative layer thickness $dr_{\perp}(t)/dt \equiv [1/H(t=0)]dH(t)/dt$, where H is the thickness of the layer, is described by

$$\left[\frac{dr_{\perp}}{dt}\right]_{\text{stress}} = \left[\frac{d\varepsilon_{\perp}}{dt}\right]_{\text{stress}} + \left[\frac{de_{\perp}}{dt}\right]_{\text{stress}} . \tag{12}$$

By using Eqs. (1) and (2) the perpendicular strains are rewritten in terms of lateral strains. In a thin film on a substrate the change of lateral plastic strain results in the opposite change of the lateral elastic strain [Eq. (4)]. According to Eq. (5) a change of lateral elastic strain is proportional to a change of lateral stress. Then the change of relative thickness by a change of stress can be written as

$$\left[\frac{dr_{\perp}}{dt}\right]_{\text{stress}} = 2\frac{1-2\nu_l}{E_l}\frac{d\sigma_{\parallel}}{dt} . \tag{13}$$

This equation is valid irrespective of the origin of the stress change. It follows that in a thin film on a substrate an increase of tensile stress results in an increase of thickness. This can be understood by realizing that in a solid with a Poisson constant smaller than $\frac{1}{2}$ the application of a tensile stress results in an increase of volume.

By use of Eq. (13) the change of relative layer thickness can be corrected for the effect of change of stress in the layer. The lateral dimensions of the layer do not change. Therefore the change of relative layer thickness is equal to the change of relative layer volume. The change rate of unconstrained relative layer volume is given by

$$\frac{dv}{dt} = \frac{dr_{\perp}}{dt} - 2\frac{1-2\nu_l}{E_l}\frac{d\sigma_{\parallel}}{dt} . \tag{14}$$

In integrated form

$$v(t)-v(t=0) = [r_{\perp}(t)-r_{\perp}(t=0)] - 2\frac{1-2\nu_l}{E_l}[\sigma_{\parallel}(t)-\sigma_{\parallel}(t=0)] . \tag{15}$$

III. VISCOSITY AND DIFFUSION COEFFICIENT

In analogy with crystalline solids, transport in amorphous solids is considered as the outcome of the formation and movement of defects. To interpret observed volume and stress changes and diffusion in amorphous solids, here the free-volume model is adopted.[1] In the free-volume model, viscosity and diffusion coefficients are related by the free volume.

A. Annihilation of flow defects

The fractional concentration c_f of flow defects, is related to the (fractional) free volume v_f according to[7]

$$c_f = \exp\left[\frac{-\gamma v^*}{v_f}\right] , \tag{16}$$

where γ is a geometrical factor of order unity, v^* is the critical free volume (per average atomic volume) needed for a jump, and v_f is the average free volume (per average atomic volume). As-prepared amorphous solids normally have excess free volume. During annealing at temperatures below the crystallization temperature the free volume is (partly) annihilated. Hence structural relaxation. If the equilibrium flow defect concentration can be ignored, the annihilation of the flow defects can be described by a bimolecular process[8,9]

$$\frac{dc_f}{dt} = -\beta k_f c_f^2 , \tag{17}$$

where β is a constant. The jump frequency for flow defects k_f is given as

$$k_f = k_{f,0}\exp\left[\frac{-Q_f}{RT}\right] , \tag{18}$$

where $k_{f,0}$ is the attempt frequency for flow defects, Q_f is the activation energy for the movement of flow defects, and R is the gas constant. For isothermal annealing the solution of Eq. (17) is

$$\frac{1}{c_f(t)}-\frac{1}{c_f(t=0)}=\beta k_f t \ . \tag{19}$$

Or, explicitly expressed in terms of free volume [see Eq. (16)],

$$v_f(t)=\frac{\gamma v^*}{\ln\left[\exp\left[\frac{\gamma v^*}{v_f(t=0)}\right]+\beta k_f t\right]} \ . \tag{20}$$

B. Viscosity

The viscosity of an amorphous solid depends on the flow defect concentration. During annealing of amorphous solids the defect concentration changes (see above). This implies a time-dependent viscosity. Assuming Newtonian viscous flow (low shear forces) the viscosity η can be expressed as[10]

$$\eta=\frac{k_B T}{c_f k_{f,0}\Omega}\exp\left[\frac{Q_\eta}{RT}\right] , \tag{21}$$

where k_B is the Boltzmann constant, Ω is the average atomic volume, and Q_η is the activation energy for viscous flow. For isothermal annealing, with Eqs. (16), (17), and (21), it follows that

$$\frac{1}{\eta}\frac{d\eta}{dt}=\beta k_f \exp\left[\frac{-\gamma v^*}{v_f}\right] . \tag{22}$$

C. Diffusion coefficient

In analogy with the random walk theory for substitutional diffusion in crystalline solids, the diffusion coefficient of amorphous solids is given as[1]

$$D=a c_d k_d \lambda_d^2 , \tag{23}$$

where a is a geometric constant (normally taken equal to $\frac{1}{6}$, Ref. 10), c_d is the diffusion defect concentration, k_d is the jump frequency for diffusion defects, and λ_d is the diffusional jump distance. k_d is defined by

$$k_d=k_{d,0}\exp\left[\frac{-Q_d}{RT}\right] , \tag{24}$$

where $k_{d,0}$ is the attempt frequency for diffusion defects and Q_d is the activation energy for the movement of diffusion defects.

A distinction may be made between flow defects and diffusion defects. Usually the flow defect concentration c_f and the diffusion defect concentration c_d are considered to be equal. However, the relation $c_d=c_f^{1/2}$ has been proposed in Ref. 11 to correlate viscosity data presented in Ref. 9 with diffusion data reported in Ref. 12. The relation $c_d=c_f^{1/2}$ is incompatible with the data of this study; see Sec. VII A. Here the flow defect concentration and the diffusion defect concentration are considered to be equal

$$c_d=c_f \ . \tag{25}$$

From Eqs. (23)–(25) it follows that

$$D=a c_f \lambda_d^2 k_{d,0}\exp\left[\frac{-Q_d}{RT}\right] . \tag{26}$$

For isothermal annealing from Eq. (26) it can be derived (analogous to Sec. III B)

$$\frac{d(D^{-1})}{dt}D=\beta k_f \exp\left[\frac{-\gamma v^*}{v_f}\right] . \tag{27}$$

D. Relation between viscosity and diffusion coefficient

For liquids the relation between the diffusion coefficient and the viscosity is described by the Stokes-Einstein relation

$$\eta D=\frac{1}{3\pi L}k_B T , \tag{28}$$

where L is a length of the order of the atomic diameter. With the activation energy for viscous flow Q_η equal to the activation energy for diffusion Q_d (which has been observed[13]), from Eqs. (21) and (26) a relation analogous to Eq. (28) is obtained

$$\eta D=p k_B T , \tag{29}$$

where

$$p=\frac{a\lambda_d^2 k_{d,0}}{\Omega k_{f,0}} . \tag{30}$$

With $a=\frac{1}{6}$, $\lambda_d=2.4\times10^{-10}$ m (the nearest atomic distance in hexagonal $MoSi_2$), $\Omega=13.4\times10^{-30}$ m^3 (the average atomic volume of hexagonal $MoSi_2$), and $k_{d,0}=k_{f,0}$, it is found that $p=7.2\times10^8$ m^{-1}. This is close to the factor $1/3\pi L$ in Eq. (28) (taking $L=\lambda_d$ it is found that $1/3\pi L=4.4\times10^8$ m^{-1}).

In correspondence with Eq. (29), for isothermal annealing it follows from Eqs. (22) and (27)

$$\frac{1}{\eta}\frac{d\eta}{dt}=D\frac{d(D^{-1})}{dt} . \tag{31}$$

IV. ISOTHERMAL ANNEALING

Taking the derivative of η [Eq. (21)] with respect to time and substituting Eqs. (17) and (18) one obtains

$$\frac{d\eta}{dt}=\frac{\beta k_B T}{\Omega}\exp\left[\frac{Q_{\dot\eta}}{RT}\right] \tag{32}$$

where $Q_{\dot\eta}=Q_\eta-Q_f$. The dependence of Ω on the annihilation of free volume is negligible. Hence during isothermal annealing $d\eta/dt$ is time independent and thus

$$\eta(t)=\eta(t=0)+\frac{d\eta(t)}{dt}t , \tag{33}$$

which has been confirmed experimentally.[9,14]

Similarly, it follows from Eqs. (17), (18), and (26) that

$$\frac{d(D^{-1})}{dt}=\frac{\beta k_{f,0}}{a\lambda_d^2 k_{d,0}}\exp\left[\frac{Q_{D^{-1}}}{RT}\right], \tag{34}$$

where $Q_{D^{-1}}=Q_d-Q_f$. The dependence of λ_d on the annihilation of free volume is negligible. Hence during isothermal annealing $d(D^{-1})/dt$ is time independent and thus

$$D^{-1}(t)=D^{-1}(t=0)+\frac{d[D^{-1}(t)]}{dt}t, \tag{35}$$

which has been confirmed experimentally.[13,15]

V. EXPERIMENT

The interdiffusion in and the stress and thickness changes of amorphous Mo/Si multilayers were measured as a function of annealing time. For the determination by x-ray diffraction of the interdiffusion coefficient and the decrease of thickness of the amorphous Mo/Si multilayer the heat treatment was interrupted at fixed times. In separate experiments, the stress changes during heat treatment in the Mo/Si multilayer were monitored by measuring *in situ* the wafer curvature.

A. Specimen preparation

(100)-oriented Si single-crystal wafers [0.285±0.005 mm thick, 50.8 mm diameter, *p*-type (B) doped with a resistivity of 20–30 Ω cm] covered with a 50-nm SiO_2 layer were used as substrates for the amorphous Mo/Si multilayers. In addition a substrate with only a 200-nm SiO_2 layer was produced. Using a Leybold Z550 dual target sputtering apparatus in which argon was used as the sputtering gas, the SiO_2 layers were rf sputtered from a SiO_2 target (99.995 wt. %). The amorphous Mo/Si multilayers (352±6 nm thick) with a composition modulation period of about 1.2 nm were prepared by alternately dc sputtering from a Mo target (99.9 wt. %) and rf sputtering from a Si target (99.999 wt. %). Before sputtering the base pressure was less than 10^{-5} Pa. The targets were cleaned by sputtering against a shutter for 30 min. The Mo/Si ratio of the multilayers was controlled by tuning the deposition rates of Mo and Si. After deposition the composition of the specimens was determined by applying electron-probe microanalysis as 33.20±0.11 at. % Mo, 65.66±0.36 at. % Si, and 1.13±0.05 at. % Ar, which is equivalent to a [Mo]/[Si] ratio of 0.5.

Specimen *A*, used for the interdiffusion measurements, was cut from the middle of the substrate wafer along the [110] direction of the substrate to a width of 26 mm. The wafers of specimen *B* (with Mo/Si multilayer) and specimen *C* (200-nm SiO_2 layer only), both used for the *in situ* stress measurements, were not reduced in size.

B. Heat treatment

The heat treatment of specimen *A* was performed in an Ar atmosphere in a horizontal furnace equipped with a 30-mm-diam fused silica tube. Before entrance in the furnace the Ar (purity 99.998%) was led through a moisture filter, a charcoal filter, and an oxygen filter (final concentration $[O_2]<1$ ppm).

Before moving the specimen into the hot zone, the tube was evacuated three times with a rotary pump and backfilled with Ar. During the heat treatment the Ar flow was kept at 50 ml min^{-1} (linear velocity 1.2 mm s^{-1}). The temperature, measured with a thermocouple inside the fused silica tube just below the specimen, was controlled within 1 K.

The as-deposited specimen *A* was heated, with an average heating rate of 1.9 K min^{-1}, up to the isothermal annealing temperature (about 523 K; see Fig. 3). During the isothermal annealing, at certain times the heat treatment was interrupted for x-ray diffraction analysis. The duration of the first isothermal anneal was 0.25 h. The next steps were chosen such that the cumulative annealing times were doubled each step up to 256 h. Thereafter two time steps of 64 h were applied.

The heat treatments for the *in situ* stress measurement (specimens *B* and *C*) were carried out in another horizontal furnace equipped with a 100-mm-diam fused silica tube. The Ar flow during these experiments was 610 ml min^{-1} (linear velocity 1.3 mm s^{-1}). Apart from an initial overshoot the temperature, measured with a thermocouple inside the fused silica tube just below the specimen, was controlled within 1 K. The heat treatments of specimen *B* and *C* were similar to the heat treatment of specimen *A* (see Fig. 3). However, these heat treatments were not interrupted for x-ray diffraction experiments. After the stress relaxation experiment of specimen *B* the specimen was additionally heated to about 750 K and isothermally annealed for 1 h. During this heat treatment the amorphous multilayer crystallized to hexagonal $MoSi_2$. The multilayer periodicity was still recognizable, therefore the volume reduction by crystallization could be obtained. In order to determine the stress-free curvature of the wafers and the elastic constants of the layer, an additional heat treatment of 1 h at 1273 K was applied to specimens *B* and *C*.

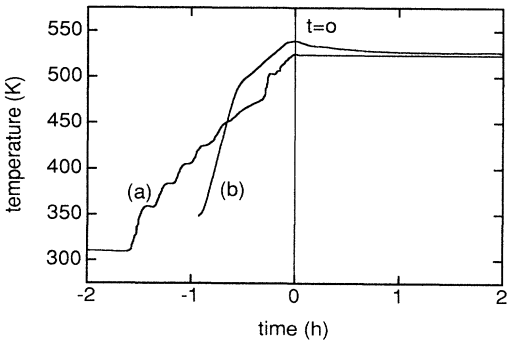

FIG. 3. Thermal histories of specimens *A* and *B*. The start of the isothermal annealing is indicated by $t=0$. (a) Temperature of specimen used for interdiffusion and thickness change measurement (the interruptions of the heat treatment for the x-ray diffusion measurements are not shown). (b) Temperature of specimen used for *in situ* stress change measurement.

C. *In situ* wafer curvature measurement: determination of film stress

An optical technique analogous to that described in Ref. 16 was used to measure *in situ* the wafer curvature of specimens B and C. The experimental setup employed has been described in Ref. 17; it has a sensitivity of about 10 MPa.

The stress in the Mo/Si multilayer on the Si substrate was calculated from the corrected radius (see below) of curvature by application of the modified Stoney equation[18]

$$\sigma_{\parallel}=\frac{E_s}{6(1-\nu_s)}\frac{d_s^2}{d_l R_{\mathrm{Mo/Si}}}\ , \tag{36}$$

where d_l is the layer thickness, d_s is the substrate thickness, $R_{\mathrm{Mo/Si}}$ is the curvature of the wafer caused by the Mo/Si multilayer, E_s is the Young's modulus of the substrate, ν_s is the Poisson constant of the substrate, and $E_s/(1-\nu_s)=182$ GPa.[19,20] For a stack of thin films on a thick substrate, the reciprocal radius of wafer curvature is the sum of the reciprocal radii of wafer curvature caused by each film.[21] Specimen B has a 50-nm-thick intermediate SiO_2 layer between the Mo/Si multilayer and the substrate. Specimen C only has a 200-nm-thick SiO_2 layer. To correct for the contribution of the intermediate SiO_2 layer to the reciprocal radius of curvature of specimen B, the measured reciprocal radius of curvature of specimen C was divided by 4 and subsequently subtracted from the measured reciprocal radius of curvature of specimen B [cf. Eq. (36)]. The resulting reciprocal radius of curvature is the contribution of the Mo/Si multilayer to the bending of specimen B.

All reciprocal radii of curvature mentioned were corrected for the stress-free curvature, which has been taken equal to the curvature of the wafer with a stress-free film as observed at 1273 K after 1 h of annealing (cf. Sec. V B). No corrections were necessary for the change of the layer thickness during the experiments.

D. X-ray diffraction analysis: determination of interdiffusion coefficient and thickness change

The interdiffusion in the amorphous Mo/Si multilayer of specimen A was studied by tracing the decay of the x-ray diffraction integrated intensity I of the first-order multilayer reflection, corresponding to the composition modulation, as a function of the annealing time t. For interdiffusion in crystalline multilayers it has been verified experimentally that[22]

$$\frac{d}{dt}\left[\ln\frac{I}{I(t=0)}\right]=\frac{-8\pi^2}{\Lambda^2}D \tag{37}$$

where Λ denotes the composition modulation period as obtained from the x-ray diffraction angle of the peak maximum of the first-order multilayer reflection. During isothermal interdiffusion, with a time-dependent diffusion coefficient according to Eq. (35) and taking Λ as a constant, the decay of the x-ray intensity is obtained by integration of Eq. (37) as

$$\ln\left[\frac{I(t)}{I(t=0)}\right]=-\frac{8\pi^2}{\Lambda^2\dfrac{d[D^{-1}(t)]}{dt}}\times\ln\left[1+\frac{d[D^{-1}(t)]}{dt}D(t=0)t\right]\ . \tag{38}$$

To determine $d[D^{-1}(t)]/dt$ and $D(t=0)$ Eq. (38) is fitted to the experimental data.

The x-ray diffraction measurements were performed applying a Siemens F-ω diffractometer, equipped with a diffracted beam graphite monochromator set to Cr $K\alpha$ radiation.

Starting with specimen A in the as-deposited condition and then after each interruption of the heat treatment, as described in Sec. V B, three diffraction experiments were performed each time.

(i) The first-order multilayer reflection was measured in the range $2\theta=9.3°-13.3°$ with steps of $\Delta 2\theta=0.005°$. To reduce errors in the measured intensity arising from the nonideality of the monochromator and to average over the surface of the specimen, oscillation of the specimen around the diffractometer axis with an amplitude of 0.5° was applied. Special care was taken to position the specimen in the diffractometer always in the same way.

(ii) A scan in the range $2\theta=30°-104°$ was measured to verify that the Mo/Si multilayer was still amorphous. An offset of 1.5° from the symmetric Bragg-Brentano specimen orientation around the diffractometer axis was applied to prevent occurrence of the "forbidden" Si(200) reflection from the monocrystalline substrate.

(iii) The intensity of the (111) reflection of a polycrystalline Si standard specimen was measured to monitor the intensity of the incident beam. In this way the measured intensity of the first-order multilayer reflection could be corrected for atmospheric pressure changes and aging of the x-ray tube.

The change of the relative multilayer thickness $r_{\perp}$ was determined from the relative change of Λ.

VI. RESULTS

A. Elastic constants

The application of Eqs. (11) and (15) involves the magnitudes of E_l and ν_l must be known. During isothermal annealing E_l and ν_l will be taken as constants.

The magnitude of $E_l/(1-\nu_l)$ is assessed from the stress change that occurred, after the isothermal annealing treatment, during cooling to room temperature by employing Eqs. (5) and (7). The value of $E_l/(1-\nu_l)$ at the annealing temperature can be somewhat different from the value at room temperature, but this effect is considered to be negligible as compared to the experimental inaccuracy.

By plotting the stress versus the temperature (Fig. 4) a straight line was obtained; from its slope it was obtained that $\Delta\alpha_{\mathrm{th}}E_l/(1-\nu_l)=1.1$ MPa K^{-1}. The difference in

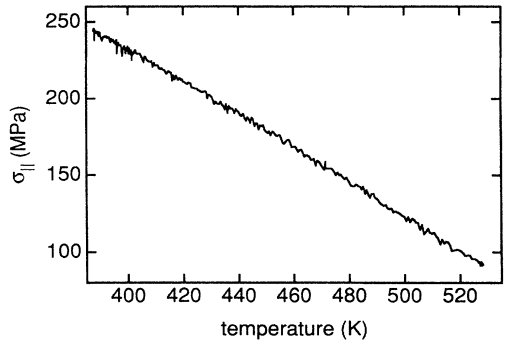

FIG. 4. Stress $\sigma_{\parallel}$ in the amorphous Mo/Si multilayer of specimen *B* vs temperature, measured during *cooling* after isothermal annealing.

linear thermal expansion coefficient between the *amorphous* multilayer and the Si substrate $\Delta\alpha_{\text{th}}$ is unknown. As a first estimate the expansion coefficient of the amorphous multilayer is taken equal to that of tetragonal[23] $MoSi_2$ (t-$MoSi_2$) and α_{Si} has been taken from Ref. 24. Averaging over the temperature range between the annealing temperature and room temperature, this leads to $\Delta\alpha_{\text{th}}=4.2\times10^{-6}\ \text{K}^{-1}$ and thus

$$\frac{E_l}{1-\nu_l}=262\ \text{GPa} . \tag{39}$$

During the heat treatment at 1273 K, described in Sec. V B, the film transformed into stress-free tetragonal $MoSi_2$, as observed by x-ray diffraction. After cooling to room temperature the difference in thermal expansion between t-$MoSi_2$ and Si caused a high thermal stress in the *crystalline* film. With the wafer curvature measurement technique described in Sec. V C, $\sigma_{\parallel}=952$ MPa was obtained. No correction was made for the change of volume of the layer during crystallization (see Sec. VII B). Using the x-ray diffraction $\sin^2\psi$ method[25] and assuming elastic isotropy (see Sec. II) it was obtained that

$$\left[\frac{E_l}{1+\nu_l}\right]_{t\text{-}MoSi_2}=\frac{\sigma_{\parallel}}{\varepsilon_{\parallel}-\varepsilon_{\perp}}=260\ \text{GPa} . \tag{40}$$

Compared to elastic constants of crystalline solids, elastic constants of amorphous solids of corresponding composition are usually smaller: the bulk modulus K about 4% and the shear modulus G about 30%.[26] For elastic isotropy the relation between shear modulus, modulus of elasticity, and the Poisson constant reads

$$2G=\frac{E}{1+\nu} . \tag{41}$$

Then, $E_l/(1+\nu_l)$ for the amorphous film can be estimated from $E_l/(1+\nu_l)$ found for t-$MoSi_2$ by reducing this value [see Eq. (40)] with 30%

$$\frac{E_l}{1+\nu_l}=182\ \text{GPa} . \tag{42}$$

From Eqs. (39) and (42) E_l and ν_l of the amorphous Mo/Si multilayer can be calculated

$$E_l=215\ \text{GPa},\quad \nu_l=0.18 .$$

These values for E_l and ν_l have been used in the analysis of the experimental stress and thickness changes.

B. Stress behavior

A schematic presentation of the stress change in a thin amorphous Mo/Si multilayer on a thick substrate during heating up to the annealing temperature and during subsequent isothermal annealing is shown in Fig. 5. During heating up to the isothermal annealing temperature, the difference in thermal expansion between layer and substrate causes a compressive stress in the layer. Volume reduction of the layer, for example, by free-volume annihilation, leads to tensile stress buildup in the layer. Apparently, during heating up, initially the buildup of compressive thermal stress is dominant, whereas later, at higher temperatures, the buildup of tensile stress as a result of volume reduction dominates. The start of the isothermal annealing, $t=0$, is marked by an abrupt change of the slope of the stress curve (see inset of Fig. 5); from this point onward no further buildup of thermal stress occurs.

On isothermal annealing beyond $t=0$ the stress is still increasing. Hence, for the time range studied the tensile stress buildup by volume reduction prevails over the stress relaxation by viscous flow and/or anelastic relaxation [cf. Eq. (11) with $dT/dt=0$].

The experimentally observed stress change of specimen *B* during isothermal annealing at 528 K is shown in Fig. 6. The drawn curve represents a fit to the stress data as described in Sec. VII F.

C. Volume behavior

The thickness changes observed during isothermal annealing at 523 K of the amorphous Mo/Si multilayer of specimen *A*, as derived from $\Delta\Lambda/\Lambda$ (cf. Sec. V D), are

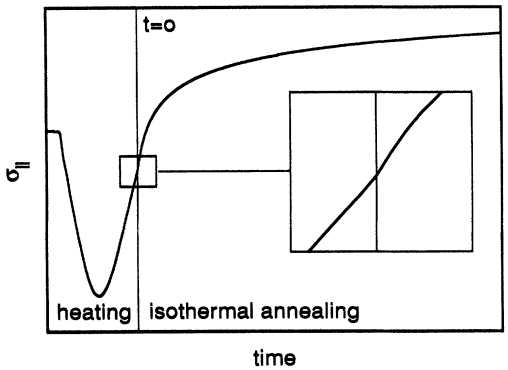

FIG. 5. Schematic representation of stress change during heating to the annealing temperature and subsequent isothermal annealing. $t=0$ indicates the start of isothermal annealing. Inset: at $t=0$ the slope of the stress curve changes discontinuously due to finished buildup of thermal compressive stress.

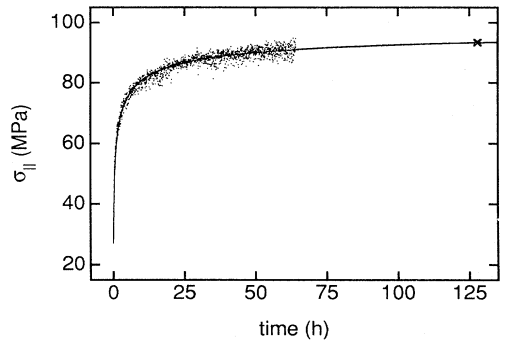

FIG. 6. Measured stress $\sigma_{\parallel}$ of specimen B vs annealing time at 528 K. The drawn curve represents the fit described in Sec. VII F. The marker (×) indicates the extrapolated data point used in Sec. VI C.

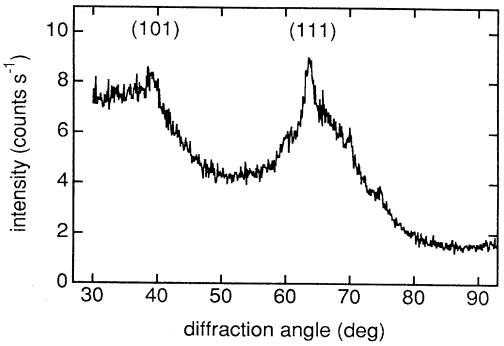

FIG. 8. Diffractogram of specimen A after isothermal annealing for 384 h at 523 K (Cr $K\alpha$, $\lambda=0.2291$ nm). The (101) and (111) reflections of hexagonal $MoSi_2$ (Ref. 27) are indicated.

shown in Fig. 7 (triangular data points). At the time of the last data point (384 h) crystallization was clearly observed (see Fig. 8), but up to 128-h annealing time crystallization was not detected. The stress measurement (specimen B) was conducted for only about 64 h and is therefore not disturbed by crystallization.

The unconstrained volume change can be obtained from the thickness change (specimen A) and the stress change (specimen B) by use of Eq. (15). During heating up to the annealing temperature free-volume annihilation already occurs. Therefore, if measurements of specimen A and B are to be used together, the thermal histories of both specimens ideally should be the same. The specimens have been prepared simultaneously. Hence the as-deposited states of both specimens are considered to be equal, but as can be seen from Fig. 3 the thermal histories of specimens A and B differ and, strictly speaking, the requirement for the application of Eq. (15) is not fulfilled. However, with the Poisson constant and modulus of elasticity of the amorphous multilayer as obtained in Sec. VI A, the relative thickness change due to the stress change [see Eq. (15)] only amounts to 6×10^{-6} per MPa stress change. Therefore the difference in thermal history between specimens A and B does not significantly affect the results obtained by use of Eq. (15). Further, during annihilation of free volume the modulus of elasticity of amorphous solids can change as much as 10%.[28] Again, as above, the correction to the thickness change is small [see Eq. (15)] and thus a changing modulus of elasticity will not affect significantly the calculated volume change. Stress data are available up to 64-h annealing time (Fig. 6), whereas reliable thickness data are available up to 128-h annealing time (Fig. 7). In order to make full use of the thickness data a stress data point at 128 h has been obtained by extrapolating the fit to the stress change (see Fig. 6 and Sec. VII F). The unconstrained volume change as obtained by use of Eq. (15) is shown in Fig. 7 (bold data points).

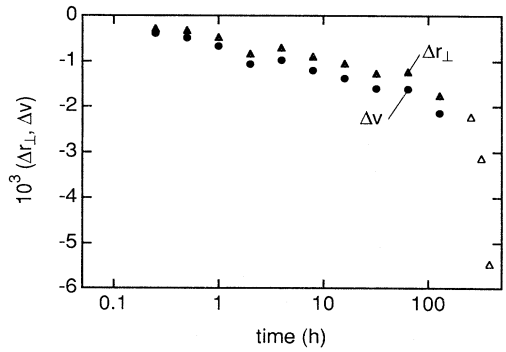

FIG. 7. Relative thickness change $\Delta r_{\perp}=r_{\perp}(t)-r_{\perp}(t=0)$ of specimen A vs the logarithm of annealing time (solid triangles). After 256 h the onset of crystallization causes additional volume decrease (open triangles). The dots represent the unconstrained relative volume change $\Delta v=v(t)-v(t=0)$ as calculated from the relative thickness change and the stress change by use of Eq. (15).

D. Interdiffusion behavior

From specimen A the first-order multilayer reflection was measured as a function of the annealing time at 523 K. The logarithm of the relative integrated intensity is plotted versus the logarithm of the annealing time in Fig. 9. To prevent any effect of crystallization of the multilayer on the determination of fit parameters, the open data points were excluded from the subsequent analysis (cf. Sec. VI C).

The drawn curve in Fig. 9 represents the least-squares fit of Eq. (38) to the bold data points. Clearly Eq. (38) provides a good description of the experimental data. Hence, in these Mo/Si multilayers the time dependence of the interdiffusion coefficient in the amorphous multilayer is well described by Eq. (35). From the fit it is obtained

$$D(t=0)=2.3\times10^{-24}\ \mathrm{m^2\,s^{-1}}$$
$$\frac{d(D^{-1})}{dt}=5.9\times10^{20}\ \mathrm{m^{-2}}\ . \qquad (43)$$

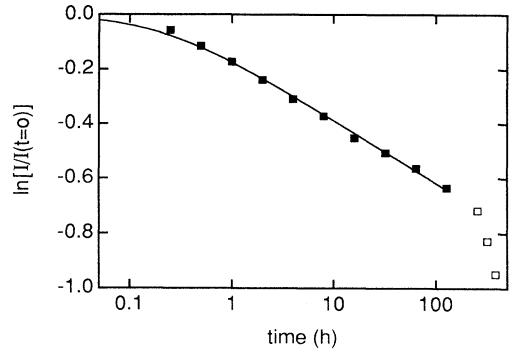

FIG. 9. Logarithm of the relative integrated intensity of the first-order multilayer reflection vs the logarithm of the isothermal annealing time (solid squares). After 256 h the onset of crystallization causes an additional decrease of intensity (open squares). Drawn curve, fit of Eq. (38) to the *solid* data points with the parameters from Eq. (43).

VII. DISCUSSION

The description of the interdiffusion coefficient in terms of the free-volume model plays an important role in the forthcoming analysis of the unconstrained volume change and the stress change. Therefore, at first the observed interdiffusion behavior will be analyzed in more detail.

In principle the volume of an unconstrained amorphous Mo/Si multilayer can change by several causes: (i) change of average atomic volume due to mixing of Mo and Si, (ii) release of argon initially incorporated during sputter deposition of the film, and (iii) annihilation of free volume. It will be shown that the volume change observed can be interpreted as a change of free volume only. From the fit parameters found, the kinetics of the flow defect annihilation can be deduced. The effect of ignorance of the equilibrium defect concentration [see Eq. (17)] on the results will be discussed.

By use of Eq. (11) and knowledge about the dependences on time of the viscosity and the anelastic relaxation in amorphous solids, the observed stress change will be interpreted. The consequences of a possible occurrence of anisotropy in the volume change of the multilayer will be discussed. The relation between the obtained viscosity and diffusion coefficient will be compared to the Stokes-Einstein relation. Finally a comparison with results obtained in other investigations will be made.

A. Details of interdiffusion behavior; relation between c_d and c_f

From previous interdiffusion measurements at 524 K in as-deposited amorphous Mo/Si multilayers with $\Lambda \approx 0.77$ nm and a [Mo]/[Si] ratio of about 0.6,[15] which is very much alike the multilayers of the present investigation (see Sec. V A), it was obtained that $D(t=0)=40\times10^{-24}$ m^2 s^{-1} and $d(D^{-1})/dt=8\times10^{20}$ m^{-2}. As compared to the present data [Eq. (43)] the difference in the initial interdiffusion coefficients must be ascribed to the difference in thermal history of the specimens. In the present investigation the specimen was slowly heated (see Fig. 3) to the isothermal annealing temperature. No such "pre-anneal" occurred in the experiment reported in Ref. 15. During the pre-anneal treatment the interdiffusion coefficient already decreases as a consequence of the annihilation of free volume. Hence, as observed, $D(t=0)$ is smaller for the present study. As expected, $d(D^{-1})/dt$ is not much affected by the pre-anneal treatment. The small difference observed may be related to the difference in overall composition between the multilayers concerned.

Interdiffusion in Mo/Si multilayers with *crystalline* Mo sublayers and amorphous Si sublayers ([Mo]/[Si] ratio about 1.3, periodicity distance Λ ranging from 3.8 to 7.5 nm) annealed at temperatures between 674 and 874 K was investigated.[29] Although these Mo/Si multilayers were not completely amorphous and of different composition, it will be assumed that the interdiffusion is comparable with the interdiffusion in completely amorphous multilayers as used in the present study. It was found[29] that

$$D=2.0\times10^{-16}\exp\left[\frac{-105\pm5}{RT}\text{kJ mol}^{-1}\right]\text{m}^2\text{s}^{-1}\ . \quad (44)$$

At 523 K, the present annealing temperature, $D=6.5\times10^{-27}$ m^2 s^{-1}. The data were obtained from that part of the interdiffusion measurements where the interdiffusion coefficient has become time independent. This is interpreted as that the equilibrium defect concentration has been attained. Compared to the value of $D(t=0)$ of the present investigation [see Eq. (43)] this diffusion coefficient is much smaller. Obviously the equilibrium defect concentration in the multilayers of Ref. 29 is much smaller than the defect concentration at $t=0$ in the multilayers of this study. An estimation of the equilibrium interdiffusion coefficient in this study is obtained from the data at the end of the isothermal annealing. According to Eq. (37), for any time, the slope of $\ln[I(t)/I(t=0)]$ versus annealing time is proportional to the diffusion coefficient. With the intensity data of Fig. 9 and Eq. (37) the experimental interdiffusion coefficient at 128 h has been calculated: $D(t=128\text{ h})=5.3\times10^{-27}$ m^2 s^{-1}. Indeed, this value of the diffusion coefficient is close to the equilibrium diffusion coefficient obtained from Ref. 29 [see Eq. (44)].

The interdiffusion coefficient in Eq. (43) was obtained by use of Eq. (38), on the basis of $c_d=c_f$. If the relation $c_d=c_f^{1/2}$ is applied to describe the interdiffusion coefficient (cf. Sec. III C), again taking Λ as a constant, the decay of the x-ray intensity is obtained by integration of Eq. (37) as

$$\ln\left[\frac{I(t)}{I(t=0)}\right]=\frac{16\pi^2}{\Lambda^2 CD'(t=0)}\times\{1-\sqrt{1+C[D'(t=0)]^2t}\}\ , \quad (45)$$

where $C=\beta k_f/a^2k_d^2\lambda_d^4$ and $D'(t=0)$ is the diffusion coefficient at $t=0$. According to Eq. (37) the slope of $\ln[I(t)/I(t=0)]$ versus annealing time is proportional to the diffusion coefficient, irrespective of the relation between c_d and c_f. Therefore proper fits to the intensity

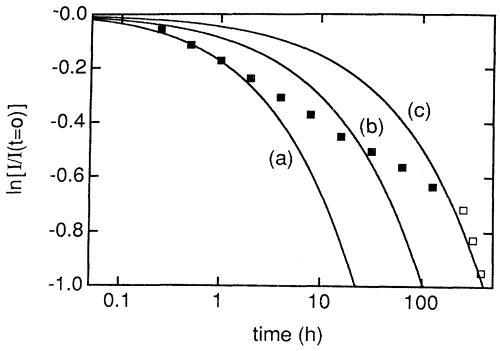

FIG. 10. Same as Fig. 9. Drawn curves, simulations of the logarithm of the relative integrated intensity of the first-order multilayer reflection vs the logarithm of the isothermal annealing time on the basis of Eq. (45) with (a) $C=1\times10^{45}$ s m^{-4}, (b) $C=5\times10^{45}$ s m^{-4}, and (c) $C=2\times10^{46}$ s m^{-4}.

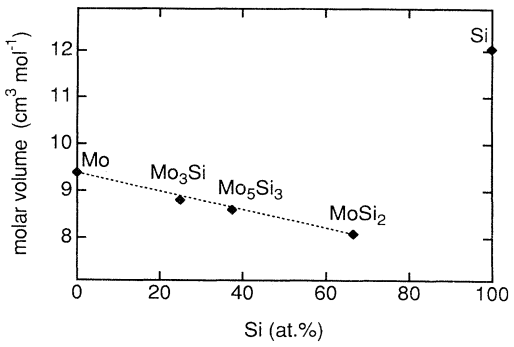

FIG. 11. Molar volume (defined as the volume of 1 mol Mo_xSi_{1-x}) of known crystalline phases in the Mo-Si system.

data of Fig. 9 [with either Eq. (38) or (45)] should give diffusion coefficients of comparable magnitude. Since with Eq. (38) a good description of the change of integrated intensity with annealing time was obtained (see Fig. 9), $D'(t=0)$ to be used with Eq. (45) must be about equal to $D(t=0)$, i.e., the one to be used with Eq. (38). In Fig. 10 the calculated logarithm of the relative integrated intensity is plotted for three different values of C, while the value of the initial diffusion coefficient $D'(t=0)$ was kept equal to $D(t=0)$ as given in Eq. (43). Clearly, Eq. (45) does not at all satisfy the experimental data.

Apart from the present investigation, in three other investigations the reciprocal diffusion coefficient was found to increase linearly with time.[13,15,30] This is in accordance with the free-volume model if c_d is proportional to c_f. The results mentioned have been obtained from amorphous multilayers prepared by sputter deposition on a substrate. Thus far, the observations leading to the proposal that c_d would be equal to $c_f^{1/2}$ have been obtained from melt quenched amorphous solids.[11,31,32] This suggests that the validity of a relation between c_d and c_f may depend on the preparation method and/or the nature of the specimen.

B. Change of molar volume

The molar volume of an amorphous phase differs only slightly from the molar volume of the corresponding crystalline phase. In this section the change of molar volume (here defined as the volume of 1 mol Mo_xSi_{1-x}) with composition will be considered. For this purpose the molar volume of the amorphous phase can be taken equal to the molar volume of a crystalline phase of corresponding composition. In Fig. 11 the molar volumes[33] of the known crystalline phases in the Mo-Si system are presented. Up to the $MoSi_2$ composition the molar volume of crystalline Mo-Si phases is almost linear with the Si concentration. For Si concentrations between $MoSi_2$ and Si the change of the molar volume with the Si concentration is unknown. The slope of the straight line through the molar volumina of Mo-Si compounds up to the $MoSi_2$ composition differs very much from that fixed by the molar volumes of pure Mo and pure Si; hence alloying of *pure* Mo and *pure* Si leads to a considerable decrease of volume. In the following, a number of considerations (a)–(c) make likely that the change of volume observed *cannot* be ascribed to such a change of molar volume.

(a) If the as-deposited multilayer, with an average composition $MoSi_2$, is conceived as a stack of alternating layers of pure Mo and pure Si, then, during homogenization by interdiffusion a pronounced volume decrease of 28% must be expected. However, with an actual composition modulation period of about 1.2 nm, the assumption of initially pure sublayers is very unrealistic. The following observations indicate a small composition modulation amplitude for the as-deposited multilayer: (i) The second-order multilayer reflection was very weak and no multilayer reflection of higher order could be detected. (ii) For a perfect Mo/Si multilayer with composition and periodicity as used in the present investigation the x-ray first-order multilayer reflection was simulated.[34] It was found that the experimentally observed intensity of this multilayer reflection, relative to the intensity in the 2θ region of total reflection, corresponds to a sinusoidal composition modulation amplitude of only about 2 at. %. (iii) From thickness and stress measurements of as-deposited and crystallized (to h-$MoSi_2$) specimens the volume reduction of the layer upon crystallization is estimated to be only about 4% (see Sec. V B). These results (i)–(iii) indicate that the as-deposited multilayer is better conceived as an almost homogeneous layer with composition modulation of small amplitude rather than as an alternating stack of pure Mo and pure Si sublayers.

(b) Defining the average diffusion distance as $\sqrt{\bar{D}t}$, with $\bar{D}$ the time-averaged diffusion coefficient, the average diffusion distance after 128 h (last data point used for fitting, Fig. 9) is only 0.1 nm. On top of the above evidence for an already small initial amplitude of the composition modulation this emphasizes that alloying, and thus a molar volume change, on annealing is limited.

(c) If the change of molar volume with Si content is linear for Si concentrations near the concentration corresponding with $MoSi_2$ [cf. (a) and see Fig. 11], no change

of volume on mixing will occur.

From points (a)–(c) discussed above it is concluded that a change of molar volume did not contribute significantly to the observed volume change.

C. Loss of argon

During sputter deposition 1.1 at. % argon is incorporated in the amorphous multilayer (cf. Sec. V A). If during annealing some of this argon could escape from the multilayer this would affect the multilayer volume.

If the diffusion coefficient of argon in the multilayer is of comparable magnitude as the Mo/Si interdiffusion coefficient, then the averaged diffusion distance is so small that loss of argon by diffusion can be ruled out; see point (b) Sec. VII B. Moreover, it was verified that the concentrations of argon as measured by electron probe microanalysis before and after the heat treatment are the same within the experimental error (0.05 at. %).

D. Annihilation of free volume

In the preceding sections it has been shown that a volume change due to release of argon from the multilayer or to a change of average atomic volume by alloying of Mo and Si can be neglected. Therefore, in the following the observed unconstrained volume change (see Fig. 7) is interpreted as a free-volume change.

Equation (20) describes the free volume as a function of time. Three parameters must be known for its calculation: $v_f(t=0)$, γv^*, and βk_f. The accuracy and number of the volume change data (see Fig. 7) is insufficient to determine these three parameters simultaneously by fitting. By use of Eq. (27) and the diffusion coefficient data for $t=0$ [see Eq. (43)] one can eliminate βk_f from Eq. (20) and $v_f(t=0)$ and γv^* remain as parameters to be fitted.

An iterative procedure according to the Simplex algorithm[35] was applied to obtain the best set of fit parameters. The solution obtained corresponds with a (local) minimum found for the (weighted) χ^2 sum as a function of the fit parameters. The resulting parameters $v_f(t=0)$ and γv^* have been given in Table I and the fitted curve has been plotted in Fig. 12 [curve (a)].

In comparing the fit results for $v_f(t=0)$ and γv^* with estimations for $v_f(t=0)$ and γv^* reported in the literature, the present data are of proper magnitude. γv^* is reported to be about 0.1,[14,36] and for v_f in the as-prepared state values of about 0.01 are expected.[36]

In Eq. (17) the term βk_f serves as the rate constant for flow defect annihilation. In Table II values for βk_f, calculated by use of Eq. (22) or (27) from literature data, have been listed together with the value of βk_f found here. Clearly the rate constant values for different amorphous solids differ enormously.

Thus far it was assumed that the flow defect concentration in the amorphous layer was far from equilibrium; cf. Eq. (17). If this is not the case the annihilation of flow defects may be described by[37]

$$\frac{dc_f}{dt} = -\beta k_f (c_f - c_{f,\mathrm{eq}})^2 , \tag{46}$$

TABLE I. Free-volume model parameters as obtained by fitting Eq. (20) to the unconstrained volume change data of specimen B (see Fig. 7), with $d(D^{-1})/dt\, D(t=0) = 1.36\times10^{-3}$ s^{-1} (see text). $c_f(t=0)$ and βk_f are derived using the equations indicated.

Fitted	$v_f(t=0)$	7.2×10^{-3}
	γv^*	0.124
Eq. (16)	$c_f(t=0)$	3.1×10^{-8}
Eq. (27)	βk_f	$4.4\times10^{4}\ s^{-1}$

where $c_{f,\mathrm{eq}}$ is the equilibrium flow defect concentration. By integration it follows that

$$\frac{1}{c_f(t)-c_{f,\mathrm{eq}}} - \frac{1}{c_f(t=0)-c_{f,\mathrm{eq}}} = \beta k_f t . \tag{47}$$

Now, the effect of the occurrence of an equilibrium defect concentration on the free-volume change will be investigated. The change of the free volume with annealing time follows from Eqs. (47) and (16). To calculate the flow defect concentration c_f as a function of annealing time according to Eq. (47) the values of $c_f(t=0)$, $c_{f,\mathrm{eq}}$, and βk_f are needed. It will be assumed that, for $t=0$, $c_{f,\mathrm{eq}}$ in Eqs. (46) and (47) can be ignored with respect to $c_f(t=0)$. Then $c_f(t=0)$ and βk_f from Table I can be applied.

The effect of an equilibrium flow defect concentration on the volume change is assessed as follows: For an adopted $c_{f,\mathrm{eq}}$ which is equivalent to an adopted $v_{f,\mathrm{eq}}$, c_f is calculated from Eq. (47) and from this, by use Eq. (16), the volume change $v_f(t)-v_f(t=0)$ is calculated. Equilibrium flow defect concentrations up to 1.7×10^{-11} corresponding to equilibrium free volumes up to 5×10^{-3} do not give rise to appreciable changes [see Fig. 12, curve (b)]. For higher equilibrium flow defect concentrations the calculated free-volume change deviates increasingly from the observed volume change at the end of the annealing treatment [see Fig. 12, curve (c)]. The maximum

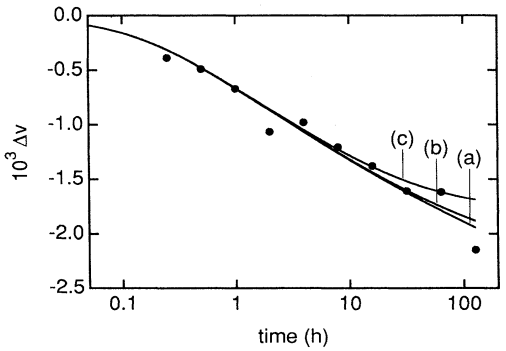

FIG. 12. The relative volume change $\Delta v = v(t) - v(t=0)$ as a function of annealing time according to the free-volume model. (a) Fit of Eq. (20) (see Table I); equilibrium defect concentration ignored, see Eq. (19). (b) Simulation on the basis of Eq. (47) with equilibrium defect concentration corresponding to $v_{f,\mathrm{eq}} = 5.0\times10^{-3}$. (c) Same as (b) with $v_{f,\mathrm{eq}} = 5.4\times10^{-3}$.

TABLE II. Values of βk_f at 523 K.

System	Specimen type	Measured phenomenon	βk_f (s^{-1})	Reference
$Fe_{40}Ni_{40}B_{20}$	ribbon	viscous flow	1.7	9
$Pd_{82}Si_{18}$	ribbon	viscous flow	2×10^5	14
$Fe_{50}Ti_{50}$	multilayer	diffusion	6.5×10^5 [a]	30
$Pd_{40}Ni_{40}P_{20}$	ribbon	viscous flow	2.4×10^9	32
$Mo_{33}Si_{66}$	multilayer	diffusion	4.4×10^4	This work

[a]Extrapolated from measurements at 433–473 K.

amount of equilibrium free volume which is compatible with the measurements is therefore considered to be equal to 5×10^{-3}. For this maximal $v_{f,\mathrm{eq}}$ the ratio of $c_{f,\mathrm{eq}}$ and $c_f(t=0)$ equals 5×10^{-4}. This demonstrates that indeed at $t=0$, $c_{f,\mathrm{eq}}$ in Eqs. (46) and (47) can be ignored with respect to $c_f(t=0)$, as was assumed above. It is concluded that for the present investigation the effect of equilibrium defect concentrations up to 1.7×10^{-11} can be ignored.

E. Stress change

Equation (11) provides a general description of the stress change in a thin film on a substrate. In Sec. VI A the elastic constants of the layer have been determined already. Since the measurements were performed isothermally, the term accounting for thermal misfit strains can be discarded. If the strain by anelastic relaxation is left out of Eq. (11), the viscosity as a function of time can be calculated, since $\sigma_\parallel$ (see Fig. 6) and the unconstrained volume change (see Fig. 7) are known as a function of time. It is noted that this viscosity is a phenomenological viscosity: in addition to actual viscous flow it may account for anelastic relaxation. In order to obtain relevant derivatives with respect to time, for the volume change use has been made of Eq. (20) and the data of Table I, and for the stress change the smooth curve of Fig. 6 was used.

The phenomenological viscosity thus obtained has been drawn as a function of time in Fig. 13. As can be seen, the phenomenological viscosity does *not* depend linearly on time. This indicates that either the actual viscous flow does not behave as described by the free-volume model [see Eq. (33)] and/or that anelastic relaxation does occur. To investigate this, the behavior of the viscosity will now be described in agreement with the free-volume model and it will be verified if the stress changes according to Eq. (11) are compatible with anelastic relaxation. The stress change to be accommodated by anelastic relaxation should at least increase continuously with time. (Under a constant stress this requirement is obvious. Note that in the present investigation during annealing the stress even increases.)

In the free-volume model [Eq. (33)] the viscosity is described with $\eta(t=0)$ and $d\eta/dt$. In Sec. III D, for isothermal annealing, Eq. (31) was derived. Then, since the time-dependent diffusion coefficient has been determined already (see Sec. VI D), only one viscosity parameter needs to be determined. The stress change to be accommodated by anelastic relaxation follows from the difference between the measured stress change and the calculated stress change from viscous flow and volume change [cf. Eq. (11)]. For very high $\eta(t=0)$ hardly any viscous flow will occur. This implies that the stress change to be accommodated by anelastic relaxation then practically equals the difference between the measured stress change and the stress change calculated from the

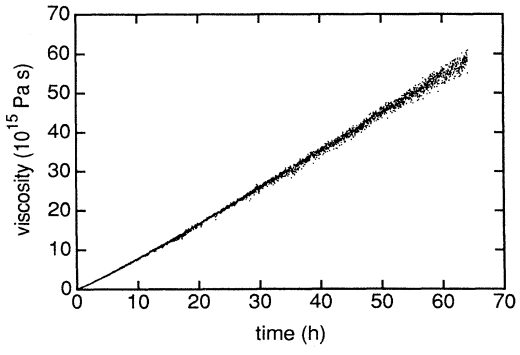

FIG. 13. Phenomenological viscosity as a function of annealing time as obtained with Eq. (11) from the stress change (Fig. 6) and the volume change [Fig. 12, curve (a)].

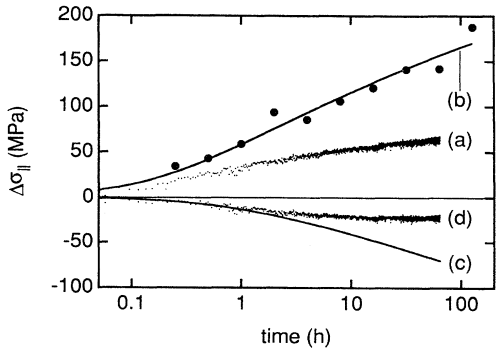

FIG. 14. (a) Measured stress change with respect to stress at $t=0$ (Fig. 6). (b) Stress change calculated from the (isotropic) volume change [Fig. 12, curve (a)]. (c) Stress change by viscous flow [$\eta(t=0)=2.2\times10^{14}$ Pa s, $d\eta/dt=3.0\times10^{11}$ Pa; Sec. VII E]. (d) Stress change to be accounted for by anelastic relaxation as obtained from (see Sec. II E) (d)=(a)−(b)−(c).

volume change. If the value for $\eta(t=0)$ is lower, then, according to Eq. (31), the value for $d\eta/dt$ is lower too. This results in more (actual) viscous flow and less anelastic relaxation. The stress change to be accommodated by anelastic relaxation should increase with time; see above. In this way, a minimal value can be found for $\eta(t=0)$ (and for $d\eta/dt$) that results in the smallest amount of stress change attributable to anelastic relaxation [see Fig. 14, curve (d)]. The minimal value obtained is $\eta(t=0)=2.2\times10^{14}$ Pa s, and using the values of $D(t=0)$ and $d(D^{-1})/dt$ as given in Eq. (43), the corresponding minimal value of $d\eta/dt=3.0\times10^{11}$ Pa; cf. Eq. (31).

A comparison of results derived from measurements on different amorphous solids is always hampered by differences occurring in thermal history. The viscosity change rate, however, is annealing time independent and it can therefore be compared more easily. Since no other results of viscosity measurements on amorphous Mo/Si multilayers are available, only a comparison can be made with data obtained from different amorphous solids. At 523 K, for $Pd_{82}Si_{18}$ we have $d\eta/dt=2\times10^{10}$ Pa (Ref. 14) and for $Fe_{40}Ni_{40}B_{20}$ we have $d\eta/dt=9\times10^{10}$ Pa.[9] In this investigation it was assessed for $Mo_{33}Si_{66}$: $d\eta/dt\geq3.0\times10^{11}$ Pa.

F. (An)isotropy of volume change

The discrepancy between measured stress change and calculated stress change as a result of annihilation of free volume and viscous flow was interpreted in the preceding section as caused by anelastic relaxation. An alternative explanation for this discrepancy can be the anisotropy described here. Thus far in this work the dimensional change of an unconstrained amorphous layer due to a volume change was supposed to be isotropic. However, in melt quenched $Fe_{40}Ni_{40}B_{20}$ anisotropic length changes on annealing have been reported.[38] Also in view of the multilayer structure, isotropy is not obvious. If a volume change would not be realized in an isotropic way, the corresponding change of strain in the layer will be different from that given by Eq. (8).

By replacing the factor $\frac{1}{3}$ in Eqs. (8) and (11) by a factor α, this anisotropy can be accounted for. With this modification the volume change is still rotational symmetric with respect to the surface normal and the stress change due to volume change is still proportional with dv/dt. The factor α can vary between 0 and $\frac{1}{2}$: $\alpha=0$ means that no change of unconstrained lateral dimensions occurs at all and that the volume change is realized fully by a thickness change; $\alpha=\frac{1}{2}$ implies that a change of the unconstrained lateral dimensions entirely accommodates the volume change.

A fit of Eq. (11), without thermal and anelastic strain terms, in principle allows the (additional) determination of the anisotropy parameter α. To this end, the volume change has been described in terms of the free-volume model (see Sec. VII D) and the viscosity has been described according to Eq. (33), using Eq. (31), with the diffusion data from Eq. (43). A good fit to the measured stress data was obtained with $\alpha=0.23$, $\eta(t=0)=2.9\times10^{14}$ Pa s and $d\eta/dt=4.0\times10^{11}$ Pa (see drawn curve in Fig. 6). The value of α found implies that, as compared to isotropic behavior, the decrease of volume of the multilayer is preferentially realized as a thickness change. If such anisotropy occurs, this is expected since thickness changes are not constrained by the substrate and lateral tensile stresses will not favor shrinkage in lateral directions. Comparing the viscosity data derived above with the minimal values found in Sec. VII E, it follows that the two sets of viscosity data differ only by a factor of 1.2.

The present investigation does not allow preference in the interpretation of the observed stress and thickness changes for either the occurrence of anelastic relaxation or the occurrence of anisotropy of volume change.

G. Relation between viscosity and diffusion coefficient

In the preceding sections proportionality of viscosity and reciprocal diffusion coefficient has been implied according to Eq. (31). The magnitude of the corresponding proportionality factor has not yet been determined. With the time-dependent diffusion coefficient according to Eq. (43) and the time-dependent viscosity from Sec. VII E, from Eq. (29) it is obtained that $p\geq7.1\times10^{10}$ m^{-1}. The minimal value of p is found to be about 100 times larger than the estimate given in Sec. III D, assuming $k_{d,0}=k_{f,0}$. If anisotropy of the volume change, instead of anelastic relaxation, would occur (see Sec. VII F), p is found to be about 130 times the value given in Sec. III D. Also, from viscosity measurements on $Pd_{82}Si_{12}$ glass[14] and from interdiffusion measurement on $Pd_{85}Si_{15}/Fe_{85}B_{15}$ multilayers[13] analogous results were obtained: the product of viscosity and diffusion coefficient was found to be much larger (160 to 590 times) than $k_BT/3\pi L$; cf. Eq. (28).[39]

These results suggest, as already proposed in Ref. 40, a transport mechanism in which many diffusional jumps may occur for each flow jump. In terms of Eq. (29) and (30), $k_{d,0}$ is much larger than $k_{f,0}$.

H. Comparison with other work

In Ref. 41 measurements of the annealing-induced stress change in amorphous $Pd_{79}Si_{21}$ films on fused silica substrates were reported. The stress change was interpreted as a result of viscous flow only [cf. Eq. (10)]. That interpretation seemed plausible since the measured stress was compressive and continuously decreasing in magnitude. However, viscous flow only is incapable to explain a buildup of tensile stress as observed in this investigation (see Fig. 6). Therefore the model presented in Ref. 41 is too simple; it may only be applicable if it has been ascertained that no volume changes and/or anelastic relaxation occurs. The reported deviation of the activation energy for $d\eta/dt$ as compared to other experimental data (on $Pd_{80}Si_{20}$) is an indication that processes other than viscous flow also affect the stress change reported in Ref. 41.

I. Effect of short-range ordering

Frequently in the structural relaxation of amorphous solids two relaxation processes are distinguished:[42] (i) topological short-range ordering (TSRO), which concerns the packing efficiency of the atoms regardless their chemical nature, as described by the free-volume model, and (ii) chemical short-range ordering (CSRO), which concerns the local arrangement of the different species of atoms regardless of their packing. The kinetics of the CSRO process is relatively fast as compared to that of the TSRO process.[43]

In principle, during annealing of amorphous solids both TSRO and CSRO can influence measured properties. In the as-deposited Mo/Si multilayers, although the amplitude of the initial composition modulation is already very small (about 2 at. %; see Sec. VII B), equilibrium with respect to CSRO is probably not fully realized.

In the present investigation no indication for the occurrence of CSRO was found. The interdiffusion behavior could be well described using only the concept of TSRO. This can be understood if CSRO has reached equilibrium during the (slow) heating to the isothermal annealing temperature (523 K). An example of such fast CSRO has been observed with $Pd_{40}Ni_{40}P_{20}$: at temperatures above 525 K, CSRO was completed within 10 s.[32] Furthermore, the volume change is insensitive to CSRO.

VIII. CONCLUSIONS

The following conclusions are drawn from this work.

(i) The coupled time behaviors of stress and volume of a thin film on a thick substrate are described by Eq. (11). The unconstrained volume change is obtained by application of Eq. (14) from measured stress and layer thickness data.

(ii) The interdiffusion coefficient is obtained by tracing the x-ray diffraction intensity of the first-order multilayer reflection. The time behavior is compatible with the free-volume model for amorphous solids taking diffusion and flow defect concentrations equal.

(iii) The unconstrained volume change is described satisfactorily with the free-volume model, using the model description of the observed interdiffusion behavior [see (ii)].

(iv) The viscosity as a function of time is obtained from stress and volume data. If only volume change and viscous flow are considered as stress change mechanisms, a viscosity is found that does not correspond to the free-volume model. If also anelastic relaxation or anisotropy of volume change are considered, and using the interdiffusion behavior, a viscosity is obtained which is compatible with the free-volume model.

(v) The product of viscosity and diffusion coefficient is found to be at least 100 times the value expected from [Eq. (29)], the free-volume-model-based equivalent of the Stokes-Einstein relation. Many diffusional jumps may occur for each flow jump.

(vi) Young's modulus and Poisson's constant of the amorphous Mo/Si multilayer have been determined as $E_l = 215$ GPa and $\nu_l = 0.18$.

ACKNOWLEDGMENTS

The authors would like to thank Ir. J. F. Jongste (Centre for Submicron Technology/Delft Institute for Microelectronics and Submicron Technology, Delft University of Technology) for his assistance with the preparation of the specimens and for the *in situ* stress measurements. The authors would like to thank Ir. W. G. Sloof for the electron-probe microanalysis measurements. This research forms part of a joint project of the Centre for Submicron Technology and the Laboratory of Metallurgy. Financial support of the "Innovatiegericht onderzoekprogramma voor IC-technologie (IOP-IC)" is gratefully acknowledged.

[1] F. Spaepen, in *Physics of Defects,* Les Houches Lectures XXXV, edited by R. Balien, M. Kléman, and J.-P. Poirer (North-Holland, Amsterdam, 1981), p. 136.

[2] J. D. Lubahn and R. P. Felgar, *Plasticity and Creep of Metals* (Wiley, New York, 1961), p. 299.

[3] F. A. McClintock and A. S. Argon, *Mechanical Behavior of Materials* (Addison-Wesley, Reading, MA, 1966), Chap. 7.

[4] A. S. Argon and H. Y. Kuo, J. Non-Cryst. Solids **37**, 241 (1980).

[5] A. I. Taub and F. Spaepen, J. Mater. Sci. **16**, 3087 (1981).

[6] G. J. Leusink and A. van den Beukel, Acta Metall. **36**, 3019 (1988).

[7] M. H. Cohen and D. Turnbull, J. Chem. Phys. **31**, 1164 (1959).

[8] S. S. Tsau and F. Spaepen, in *Proceedings of the Fourth International Conference on Rapidly Quenched Metals, Sendai, 1981,* edited by T. Masumoto and K. Suzuki (Japan Institute of Metals, Sendai, 1982), p. 463.

[9] A. van den Beukel, E. Huizer, A. L. Mulder, and S. van der Zwaag, Acta Metall. **34**, 483 (1986).

[10] F. Spaepen, Acta. Metall. **25**, 407 (1977).

[11] A. van den Beukel, Scr. Metall. **22**, 877 (1988).

[12] J. Horvath, H. Mehrer, Cryst. Lattice Defects Amorph. Mater. **13**, 1 (1986).

[13] A. L. Greer, C.-J. Lin and F. Spaepen, *Proceedings of the Fourth International Conference on Rapidly Quenched Metals, Sendai, 1981* (Ref. 8), p. 567.

[14] A. I. Taub, and F. Spaepen, Acta Metall. **28**, 1781 (1980).

[15] W. G. Sloof, O. B. Loopstra, Th.H. de Keijser, and E. J. Mittemeijer, Scr. Metall. **20**, 1683 (1986).

[16] V. L. Teal and S. P. Murarka, J. Appl. Phys. **61**, 5038 (1987).

[17] J. F. Jongste, G.C.A.M. Janssen, and S. Radelaar, in *Thin Films: Stresses and Mechanical Properties II,* edited by M. F. Doerner, W. C. Oliver, G. M. Pharr, and F. R. Brotzen, MRS Symposia Proceedings No. 188 (Materials Research Society, Pittsburgh, 1990), p. 61.

[18] R. W. Hoffman, in *Physics of Thin Films,* edited by G. Hass and R. E. Thun (Academic, New York, 1966), Vol. 3, p. 222.

[19] W. A. Brantley, J. Appl. Phys. **44**, 534 (1973).

[20] *Metals Reference Book,* 5th ed., edited by C. J. Smithells and E. A. Brandes (Butterworths, London, 1976), p. 978.

[21]P. H. Townsend, D. M. Barnett, and T. A. Brunner, J. Appl. Phys. **62**, 4438 (1987).
[22]H. E. Cook and J. E. Hilliard, J. Appl. Phys. **40**, 2191 (1969).
[23]Y. S. Touloukian, R. K. Kirby, R. E. Taylor, and T.Y.R. Lee, *Thermal Expansion-Nonmetallic Solids,* Vol. 13 of *Thermophysical Properties of Matter* (IFI/Plenum, New York, 1977), p. 1198.
[24]P. J. Burkhardt and R. F. Marvel, J. Electrochem. Soc. **116**, 864 (1969).
[25]H. P. Klug and L. E. Alexander, *X-Ray Diffraction Procedures* (Wiley, New York, 1974).
[26]G. Knuyt, L. de Schepper, and L. M. Stals, Mater. Sci. Eng. **98**, 527 (1988).
[27]Joint Committee for Powder Diffraction Standards diffraction pattern 17-917 (hexagonal $MoSi_2$); a correction has been made to the spacing given there for the (101) planes to 0.3410 nm.
[28]E. Huizer, Ph.D. thesis, Delft University of Technology, The Netherlands, 1987, p. 90.
[29]H. Nakajima, H. Fujimori, and M. Koiwa, J. Appl. Phys. **63**, 1046 (1988).
[30]E. H. Chason and T. Mizoguchi, in *Science and Technology of Rapidly Quenched Alloys,* edited by M. Tenhover, L. E. Tanner, and W. L. Johnson, MRS Symposia Proceedings No. 80 (Materials Research Society, Pittsburgh, 1987), p. 61.
[31]G. W. Koebrugge, J. van der Stel, J. Sietsma, and A. van den Beukel, J. Non-Cryst. Solids **117/118**, 601 (1990).
[32]G. W. Koebrugge, Ph.D. thesis, Delft University of Technology, The Netherlands, 1991.
[33]P. Villars and L. D. Calvert, *Pearson's Handbook of Crystallographic Data for Intermetallic Phases* (ASM, Metals Park, OH, 1985), p. 2771.
[34]M. A. Hollanders and B. J. Thijsse, J. Less-Common Met. **140**, 33 (1988).
[35]M. S. Caceci and W. P. Cacheris, Byte, **9**, 340 (1984).
[36]A. van den Beukel and S. Radelaar, Acta. Metall. **31**, 419 (1983).
[37]S. S. Tsau and F. Spaepen, Acta Metall. **33**, 881 (1985).
[38]H.-R. Sinning, L. Leonardsson, and R. W. Cahn, Int. J. Rapid. Solidific. **1**, 175 (1985).
[39]A. L. Greer, J. Non-Cryst. Solids **61&62**, 737 (1984).
[40]F. Spaepen, Mater. Sci. Eng. **97**, 403 (1988).
[41]A. Witvrouw and F. Spaepen, in *Thin Films: Stresses and Mechanical Properties II* (Ref. 17), p. 147.
[42]T. Egami, J. Mater. Sci. **13**, 2587 (1978).
[43]A. van den Beukel, S. van der Zwaag, and A. L. Mulder, Acta Metall. **32**, 1895 (1984).